MARS SEASONAL CAP EDGES AND CO_2 ICE COLUMN DENSITY. T. N. Titus[1] and G. E. Cushing[1], [1]U.S. Geological Survey, Astrogeology Science Center, 2255 North Gemini Dr., Flagstaff, AZ 86001.

Introduction: Mars is a dynamic planet where 25%-30% of the predominately CO_2 atmosphere [1, 2] is annually exchanged between the atmosphere and surface CO_2 ice [3-6]. The mass of seasonal CO_2 ice has been estimated to be 3.5 x 10^{15} kg in the north and 6.5 x 10^{15} kg in the south [7]. While bulk estimates of the CO_2 mass are available in the literature from a variety of measurements, including pressure curves, high energy particles (gamma rays and neutrons) and gravity, spatial resolution of the CO_2 ice distribution has usually been limited to zonal means (and then usually making several assumptions). Insolation-mass balance calculations have also been used to estimate local column densities [e.g. 8-10]. Here we use the insolation-mass balance (IMB) approach over both seasonal caps and validate the results with comparison to the bulk mass as estimated from gravity data [7].

Data: The Mars Global Surveyor (MGS) Thermal Emission Spectrometer (TES) [11] provides near continuous monitoring of the solar albedo, planetary temperature and surface temperature over several annual cycles for both the northern and southern polar regions. As such, TES is well-suited to monitor the advancing and retreating seasonal cap edge, as well as estimate the energy balance of condensing or sublimating CO_2 ice. If the date of complete CO_2 ice sublimation is known (often referred to as the CROCUS date [8]), then the energy balance can be integrated backwards in time from that date. A more complete description can be found in [10]. This method provides a spatially resolved estimate of the CO_2 ice column density as a function of season.

The determination of the CROCUS date can be achieved either using the thermal infrared (TIR) spectral channels at 25 microns or from the solar albedo bolometer (SAB). A sudden increase in temperature of more than 5 K above the CO_2 frost temperature (~145 K) usually indicates that the CO_2 ice is no longer buffering the surface temperature. The SAB can also be used to determine the disappearance of seasonal CO_2 ice by observing a slight increase in brightness followed by an immediate darkening. For the northern seasonal cap, the TIR method is best as the seasonal CO_2 ice cap is surrounded by an annular layer of H_2O ice during much of the retreat phase. [9, 12] In the south, the SAB method is best as the warm dusty atmosphere can affect observed brightness temperatures even at 25 microns.

Results: A comparison between the northern and southern seasonal caps can provide context for assumptions about seasonal CO_2 ice deposition and sublimation.

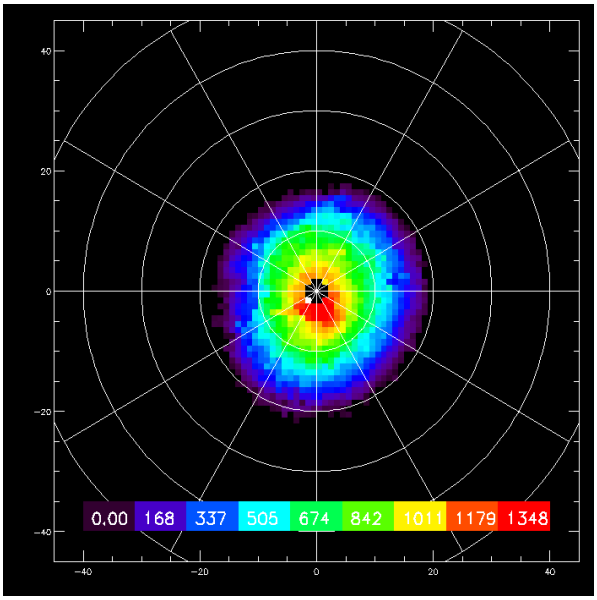

Figure 1: North polar seasonal cap column density (kg/m^2) at L_s 0°.

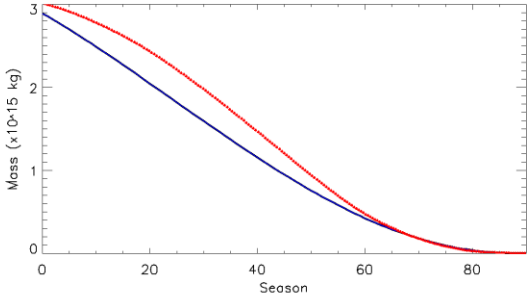

Figure 2: North polar seasonal cap mass comparison between estimates from gravity data (blue) [7] and this analysis using the IMB method (red).

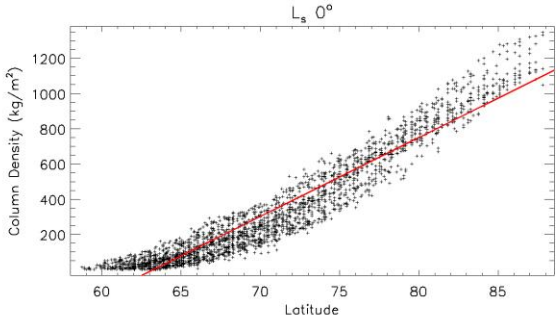

Figure 3: North polar column density at L_s 0°. The red line shows a linear fit which is the assumption made by [7] when they estimated the cap mass from gravity data.

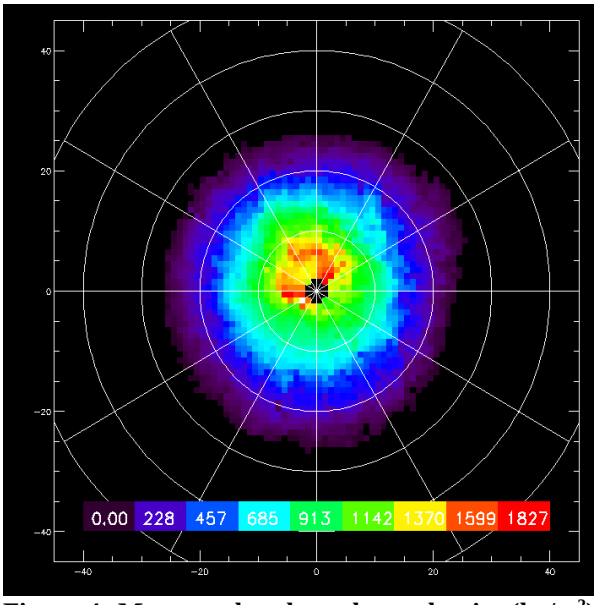

Figure 4: Mars south polar column density (kg/m^2) at L_s 205°.

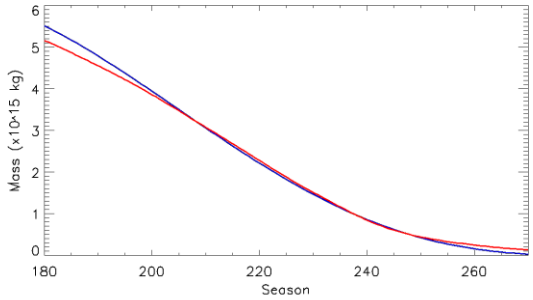

Figure 5: South polar seasonal cap mass comparison between estimates from gravity data (blue) [7] and this analysis using the IMB method (red).

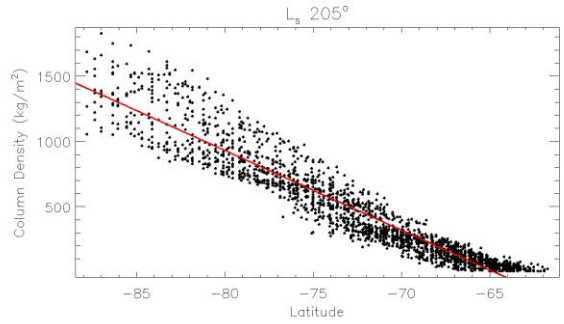

Figure 6: South polar column density at L_s 205°. The red line shows a linear fit which is the assumption made by [7] when they estimated the cap mass from gravity data.

North Polar Seasonal Cap. The northern seasonal cap is generally symmetric (Fig. 1). A comparison between the cap mass as determined by the IMB approach to the gravity approach shows results that are consistent throughout the spring (Fig. 2). The seasonal CO_2 ice distribution can be approximated by a linear fit as a function of latitude (Fig. 3), as assumed by [7]. The small asymmetric distribution north of 80°N appears to correlate with the location of the permanent cap which is composed of high thermal inertia water-ice. The residual cap is also subjected to multiple CO_2-snow storms [13, 14].

South Polar Seasonal Cap. The southern seasonal cap is generally symmetric (Fig. 4), at latitudes north of 80°S. However, poleward of 80°S the longitudinal distribution becomes very asymmetric with as much as a 60% increase in net ice deposit near the residual south polar cap (RSPC) as compared to the opposite hemisphere. Colaprete et al. [15] suggested that a wintertime N=1 atmospheric standing wave caused one region of the south polar region to have more deposition through snow (the RSPC hemisphere) while the opposite side deposition was predominately direct condensation. Cornwall & Titus [16] also found enhanced snow deposition over the RSPC. A comparison between the cap mass as determined by the IMB approach to the gravity approach (Fig. 5) shows good agreement. The seasonal CO_2 ice distribution can only be loosely approximated by a linear fit as a function of latitude (Fig. 6), as assumed by [7].

Summary: In both the north and the south, the areas with the highest net accumulation of CO_2 correlate with regions with enhanced CO_2-snowfall. This is counter intuitive as CO_2-snow, with a lower emissivity than CO_2 ice, should inhibit additional accumulation of CO_2 ice. However, the low-emissivity snow may quickly morph into porous ice with near-unit emissivity as observed by Cornwall & Titus [14, 16].

References: [1] Owen et al., 1977, JGR.82(28), 4635-4639. [2] Mahaffy et al. 2013, Sci., 341(6143), 263-266. [3] Tillman et al., 1993, JGR 98, 10963-10971. [4] Forget and Pollack, 1996, JGR, 101(E7), 16865-16880. [5] Kelly et al., 2006, JGR 111(E3), E03S07. [6] Prettyman et al., 2009, JGR 114(E8), E08005. [7] Smith et al., 2009, JGR 114, E05002. [8] Kieffer et al., 2000, JGR 105, 9653–99. [9] Kieffer & Titus 2001, Icarus 154, 162–80. [10] Titus & Cushing, 2014, 8th Intern. Conf. on Mars, #1791. [11] Christensen et al., 1992, JGR 97(E5), 7719-7734. [12] Wagstaff et al., 2008, PSS, 56, 256-265. [13] Titus et al., 2001, JGR 106, 23181–96, 2001. [14] Cornwall & Titus, 2009, JGR, 114(E2) CiteID E02003, [15] Colaprete et al., 2005, Nature 435, 184–188. [16] Cornwall & Titus, 2010, JGR, 115(E6), CiteID E06011.